frontiers in Marine Science

ORIGINAL RESEARCH
published: 06 November 2018
doi: 10.3389/fmars.2018.00410

Contraction Dynamics and Respiration of Small Single-Osculum Explants of the Demosponge *Halichondria panicea*

Lars Kumala[1,2,3,4]* *and Donald Eugene Canfield*[4]

[1] Marine Biological Research Centre, University of Southern Denmark, Kerteminde, Denmark, [2] Max-Planck Odense Center on the Biodemography of Aging, Department of Biology, University of Southern Denmark, Odense, Denmark, [3] Max Planck Institute for Demographic Research, Rostock, Germany, [4] Nordcee, Department of Biology, University of Southern Denmark, Odense, Denmark

Sponges pump large amounts of seawater through their water canal system, providing both food and oxygen to the sponge body. Sponge pumping activity may show considerable variation as a consequence of contractile behavior, which includes contraction and expansion of the exhalant opening (osculum) in regular or irregular time intervals. The present study unravels short- and long-term effects of contraction-expansion events on the respiration rate of small single-osculum explants of the demosponge *Halichondria panicea*. Based on simultaneous video-microscopic time-lapse recordings of osculum cross-sectional area (*OSA*) and projected area (*A*), combined with respiration rate measurements, we further evaluate the role of pumping activity for oxygen uptake in the explants. Pumping dynamics were expressed by cyclic contraction-expansion events of the *OSA* and *A*, including osculum closure with a mean duration of 37.5 ± $CI_{95\%}$ 13.7 min. The respiration rate of sponge explants remained relatively constant at 0.046 ± $CI_{95\%}$ 0.014 μmol O_2 h^{-1} (i.e., 7.41 μmol O_2 $h^{-1}g^{-1}$ DW_{sponge}) during contraction-expansion cycles, but with a marginal decrease of 9.6% during osculum closure. Periods of pumping cessation during osculum closure likely caused reduced oxygen levels in the sponge body, increasing the oxygen gradient between the environment and the sponge interior, allowing enhanced diffusion of oxygen across the explant surface. This is a key mechanism for balancing respiratory demands during sponge contractions. While contractile behavior is only marginally associated with decreased respiratory demands in small single-osculum *H. panicea* explants, it may control the degree of internal oxygen depletion and thereby ensure maintenance of sponge-associated microorganisms during non-pumping periods.

Keywords: respiration, osculum, contraction, pumping activity, sponge explant, oxygen

OPEN ACCESS

Edited by:
Anna Di Cosmo,
Università degli Studi di Napoli Federico II, Italy

Reviewed by:
Folco Giomi,
Università degli Studi di Padova, Italy
Michael A. Menze,
University of Louisville, United States

***Correspondence:**
Lars Kumala
kumala@biology.sdu.dk

Specialty section:
This article was submitted to Aquatic Physiology, a section of the journal Frontiers in Marine Science

Received: *13 June 2018*
Accepted: *16 October 2018*
Published: *06 November 2018*

Citation:
Kumala L and Canfield DE (2018) Contraction Dynamics and Respiration of Small Single-Osculum Explants of the Demosponge Halichondria panicea. Front. Mar. Sci. 5:410. doi: 10.3389/fmars.2018.00410

INTRODUCTION

Sponges are sedentary filter-feeding invertebrates characterized by a simple body plan composed of numerous pores (ostia) on the outer surface (exopinacoderm) and a water canal system merging into one or more exhalant openings (oscula). In sponges, water pumping is accomplished by the beating flagellum of choanocytes, which are organized in choanocyte chambers to induce water

flow (Kilian, 1952; Fjerdingstad, 1961; Larsen and Riisgård, 1994; Leys et al., 2011) for the purpose of feeding, respiration and the excretion of waste products (Bergquist, 1978). Large phytoplankton cells and other particles of >5 μm entering the canal system are retained and phagocytosed in the inhalant canal system (Reiswig, 1971b; Pile et al., 1997; Duckworth and Pomponi, 2005), while free-living bacteria and other picoplankton cells are captured by the choanocyte collar filter (Fjerdingstad, 1961; Brill, 1973; Riisgård and Larsen, 2000; Leys et al., 2011). The water flow through the complex aquiferous system oxygenates the sponge body interior, allowing oxygen to diffuse into the interior sponge cells, in addition to oxygen diffusing across the sponge surface (Bergquist, 1978), a process that may be enhanced by increasing ambient water flow (Schläppy et al., 2010b).

Sponges lack true organs, muscles (Pavans de Ceccatty, 1986, 1989) and a nervous system (Jones, 1962; Pavans de Ceccatty, 1974), but they nevertheless possess coordinated contractile behavior as a response to external (Elliott and Leys, 2007) and internal stimuli (Reiswig, 1971a). This behavior includes contraction and inflation of the sponge body as well as the inhalant (ostia) and exhalant (oscula) openings (Prosser et al., 1962; Reiswig, 1971a; Gaino et al., 1991; Nickel et al., 2006; Elliott and Leys, 2007; Strehlow et al., 2016). As a possible consequence of their contractile behavior (Reiswig, 1971a), sponges arrest their pumping activity in regular as well as irregular intervals with time scales ranging from minutes to several days (Patterson et al., 1997; Tompkins-MacDonald and Leys, 2008; McMurray et al., 2014). Reduced pumping activity has previously been linked to a decrease in sponge respiration rate (Bergquist, 1978; Hadas et al., 2008; Hoffmann et al., 2008). Pumping cessation may further result in temporal anoxia in the sponge body (Hoffmann et al., 2005b; Schläppy et al., 2007), which serves as a habitat for highly diverse microbial consortia (Taylor et al., 2007; Thomas et al., 2016).

Small single-osculum explants are well-suited for exploring the relationship between sponge physiology and contractile behavior (Kumala et al., 2017), which is difficult to assess in large sponges that may display asynchronous closure and opening of their multiple oscula (Riisgård et al., 2016). Recent studies on single-osculum explants of the demosponge *Halichondria panicea* revealed a clear relationship between osculum opening dynamics and the filtration rate (=pumping rate), where no water was pumped during periods of osculum closure (Kumala et al., 2017).

The present study aims to investigate the effect of contractile behavior on the respiration rate of single-osculum explants of the demosponge *H. panicea*. We used video-microscope observations of the osculum cross-sectional area and projected area to characterize the contraction-expansion dynamics of explants, with emphasis on temporal behavior of the explant osculum. We explored the relationship between osculum opening degree and respiration rate to evaluate the effect of pumping activity on oxygen uptake.

MATERIALS AND METHODS

Preparation and Cultivation of Sponge Explants

Experiments were performed using single-osculum explants of the demosponge *H. panicea,* which were prepared and cultivated according to Kumala et al. (2017). Explant volume (mL) was determined from the volume equation for a hemisphere ($V_{sp} = 2/3 \times \pi r^3$). Explant dry weight ($DW$, g) was estimated using the conversion equation $DW = 0.07 \times V_{sp}$ (Thomassen and Riisgård, 1995). Sponge explants ($n = 3$; *ID*1-3) were starved 24 h prior to experiments.

Measurement of Respiration Rate

The respiration rate was determined as the removal rate of dissolved oxygen (DO, μmol L^{-1}) by a sponge explant placed in a closed respiration chamber starting with well-mixed fully oxygenated (0.2 μm) filtered seawater (∼15.1 ± 0.3°C, ∼20 PSU, **Figure 1**). The DO concentration (μmol L^{-1}) was recorded using a FireStingO2 optical oxygen meter (Pyro Science, Germany) connected to a computer with Pyro Oxygen Logger® software. The optical fiber was attached to a contactless oxygen sensor spot glued to the inner wall of the respiration chamber. Prior to the experiments, oxygen sensors were calibrated against air-bubbled (100% oxygen saturation) and deoxygenated (by adding sodium dithionite) filtered seawater. Respiration chambers, including glass slides with and without (=control) a sponge explant, were submerged in a temperature-controlled water bath (**Figure 1**) to minimize temperature variations during the measurement period. Oxygen readings were recorded every 5 or 10 s and corrected for changes in temperature by Pyro Oxygen Logger® software using an external temperature sensor placed in the water bath. The respiration rate of explants (R, μmol O_2 h^{-1}) and the oxygen consumption in control chambers were determined from the decrease in DO concentration (μmol L^{-1}) in the respiration chamber (V = 29.4 mL) as a function of time using Eq. (1):

$$R = (V \times b) \quad (1)$$

where V = volume of water in experimental chamber in liter, and b = slope of the regression line for the reduction in DO (μmol L^{-1}) over time in hours (**Supplementary Figure S1**) for each 10 min interval. These respiration rates were compared with the osculum opening degree and projected area (A) of explants. We also averaged respiration rates (R, μmol O_2 h^{-1}) during periods of osculum expansion (i.e., active water pumping) and osculum closure to further evaluate the effect of pumping activity on oxygen uptake. The mean respiration rate of all measurements was standardized to both mean sponge volume (V_{sp}) and DW.

Video Time-Lapse Microscopy and Image Analysis

We combined respiration experiments with simultaneous video-microscopic observations of the explant osculum opening and projected area. Temporal variations in the osculum cross-sectional area *(OSA)* were assessed from top-view time-lapse images captured by a stereo microscope (Leica M165

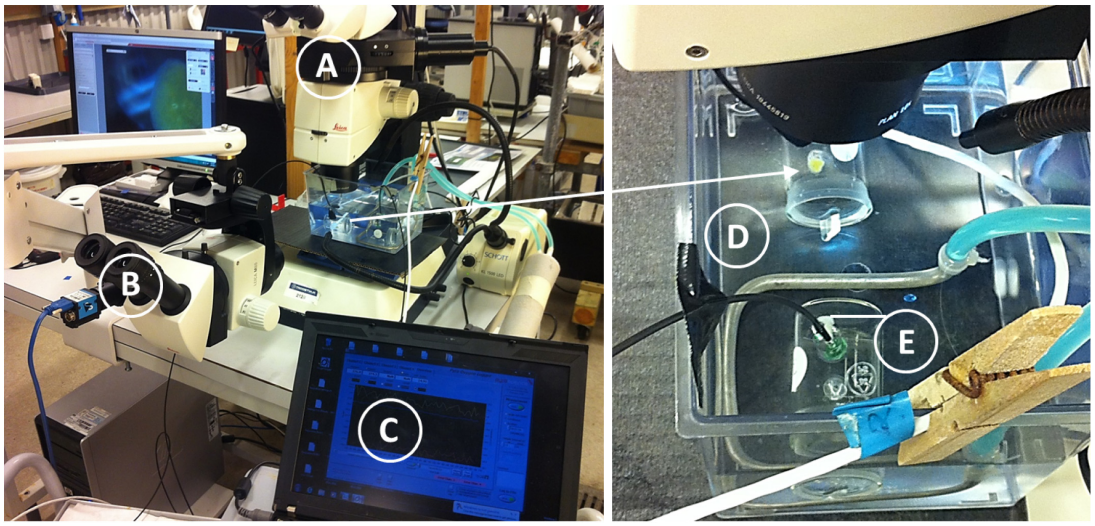

FIGURE 1 | *Halichondria panicea*. Experimental setup for video-microscopic observation of osculum from top view **(A)**, projected area from side view **(B)** and simultaneous measurements of the respiration rate **(C)** of single-osculum sponge explant in a closed respiration chamber (arrow) submerged in a temperature-controlled water bath **(D)**. A chamber with glass slide without explant served as control **(E)**. The water bath was placed on two magnetic stirrers to ensure continuous mixing in both chambers throughout the experimental period.

FC) combined with a digital camera (Leica DFC425 C). In addition, changes in the projected area (A) of explants were determined from side-view images made with a Leica M80 stereo microscope connected to an USB3.0 industrial camera (Imaging-source, DFK23UM021). Both top and side view images were simultaneously recorded every 60 s using the image acquisition software Leica Application Suite V3.8 or IC Capture 2.3, respectively.

Time-lapse images were analyzed in ImageJ (Version1.46r). The *OSA* was manually determined via pixel counts of the osculum area and subsequent conversion into mm^2 using a reference scale bar. For projected area, A, side-view image sequences were transformed to 8-bit greyscale format to convert each pixel's color information into a brightness measurement. Based on the brightness contrast between the black background and the whitish sponge, minimum and maximum threshold values were adjusted to define the pixel range covering the sponge's projected area (A). The number of pixels within the projected area was counted autonomously for each image of the image sequence and converted into mm^2 using a reference scale bar.

Contraction-Expansion Kinetics

To characterize the contraction-expansion dynamics of *H. panicea* explants, we determined speeds of contraction (C) and expansion (E) from both the changes in mean relative *OSA* ($OSA_r = OSA/OSA_{max}$) and mean relative projected area ($A_r = A/A_{max}$), where OSA_{max} (mm^2) and A_{max} (mm^2) are defined as the maximum *OSA* and projected area before each osculum closure event (cf. Nickel, 2004; Ellwanger et al., 2007). For each contraction-expansion event in both *OSA* and A, we determined the speed of contraction v_C ($\Delta OSA_r\ h^{-1}$ and $\Delta A_r\ h^{-1}$) and expansion v_E ($\Delta OSA_r\ h^{-1}$ and $\Delta A_r\ h^{-1}$) from the slope of linear models (LM) for a decrease or increase in *OSA*, or in A, over time. We further determined the duration of active water pumping Δt_P (min), i.e., $OSA > 0\ mm^2$, until osculum closure ($OSA = 0\ mm^2$) of duration Δt_C (min) at time t (min), and the time interval until subsequent osculum closure Δt (min) for each contraction-expansion cycle.

Statistical Tests

All statistical analyses were performed in R, version 3.2.0 (R Core Team, 2015). We parameterized auto-regressive models (LM; time lag: 10 min) to test for: (a) temporal changes of respiration rate R ($\mu mol\ O_2\ h^{-1}$) in response to the osculum cross-sectional area (*OSA*) (mm^2) and projected area A (mm^2) when considering individual variation (*ID*), and (b) temporal changes of respiration rate R ($\mu mol\ O_2\ h^{-1}$) in response to temporal changes in *OSA* (mm^2) and A (mm^2) when considering *ID*. We used generalized linear mixed-effect models (GLMM) in package lme 4 (Bates et al., 2015), which we parameterized with gamma error structure to test for differences between contraction and expansion speeds for OSA_r or A_r when correcting for *ID*.

RESULTS

Respiration Rates of Single-Osculum *Halichondria panicea* Explants

The overall consumption of dissolved oxygen (*DO*, $\mu mol\ L^{-1}$) is shown in **Supplementary Figure S1** for respiration chambers without (=control) and with *H. panicea* explants (*ID*1-3) throughout experimental periods of 110 h (*ID*1), 69 h (*ID*2), and 90 h (*ID*3). In total, explants had respired ∼71% (*ID*1), ∼33% (*ID*2), and ∼49% (*ID*3) of the initial *DO* (mean 271 ± 5 $\mu mol\ L^{-1}$), resulting in ∼79 $\mu mol\ DO\ L^{-1}$ (i.e., ∼28% air saturation,

*ID*1), ∼177 μmol *DO* L^{-1} (i.e., ∼63% air saturation, *ID*2), and ∼138 μmol *DO* L^{-1} (i.e., ∼49% air saturation, *ID*3) by the end of the experiments. Oxygen removal of 8 and 13% due to bacterial respiration in control chambers (**Supplementary Figure S1**) was small by comparison with oxygen consumption in chambers with explants.

Temporal changes in explant respiration rate, together with osculum cross-sectional area *(OSA)* and projected area (*A*), are shown in **Figure 2** and **Supplementary Figure S2**. Except for an initial increase in the oxygen consumption of sponge explants *ID*1 and *ID*2 (**Figure 2**), respiration rates remained relatively constant throughout the entire study period. Respiration of actively pumping ($OSA > 0$ mm^2) explants, however, decreased from 0.052 ± $CI_{95\%}$ 0.012 μmol O_2 h^{-1} to 0.047 ± $CI_{95\%}$ 0.014 μmol O_2 h^{-1} (**Table 1**) during osculum closure, thus corresponding to a relative difference of 9.6%. Neither state of the *OSA* (LM, $t = 0.128$, $P = 0.898$, see diagnostic plots in **Supplementary Figure S3**) and *A* (LM, $t = 0.260$, $P = 0.795$), nor temporal changes in *OSA* (LM, $t = 0.348$, $P = 0.701$, see diagnostic plots in **Supplementary Figure S4**) and *A* (LM, $t = 0.628$, $P = 0.530$), affected respiration rates significantly when taking into account differences among individual sponge explants. The mean (±95% confidence interval = $CI_{95\%}$) respiration rate of all measurements was 0.046 ± 0.014 μmol O_2 h^{-1}, yielding a mean volume-specific respiration rate of 0.52 ± 0.18 μmol O_2 $h^{-1}cm^{-3}{}_{sponge}$. This corresponds to a mean *DW*-specific respiration rate of 7.41 μmol O_2 $h^{-1}g^{-1}$ DW_{sponge} for single-osculum *H. panicea* explants.

Osculum Dynamics and Contraction-Expansion Kinetics

During our total observation period of 270 h (>10 days), we observed 29 contraction-expansion events among all explants ($n = 3$), which were most pronounced in changes in the *OSA* (mm^2). Each contraction-expansion event began with osculum contraction and subsequent osculum closure, i.e., $OSA = 0$ mm^2, which was followed by osculum expansion (**Figure 2**). Osculum closure was spaced in a mean (±$CI_{95\%}$) time interval of $\Delta t = 8.2 \pm 2.7$ h and lasted for a mean (±$CI_{95\%}$) duration of $\Delta t_C = 37.5 \pm 13.7$ min ($n = 29$; **Table 1**). Individual sponge explants differed in their contractile behavior, as expressed by irregular osculum contraction-expansion events in explant *ID*1 and *ID*2 compared to more frequent and regular events in explant *ID*3 (**Table 1** and **Figure 2**). For sponge explants *ID*1 and *ID*3, the maximum osculum area OSA_{max} (mm^2) decreased as a function of time and decreasing oxygen concentration in the experimental chamber (**Figure 2** and **Supplementary Figure S1**). Speeds of contraction v_C and expansion v_E of the relative osculum cross-sectional area (OSA_r) showed no significant difference (GLMM, $t = -0.824$, $P = 0.410$), reaching means (±$CI_{95\%}$) of -0.018 ± 0.015 ΔOSA_r min^{-1} and 0.022 ± 0.016 ΔOSA_r min^{-1}, respectively (**Figure 3** and **Table 1**).

Contraction-expansion events in *OSA* were accompanied by simultaneous changes in the projected area *A* (mm^2; **Supplementary Figure S2**). In most cases, temporal changes in *A* were different from the contraction-expansion events observed in *OSA*, as expressed by additional expansion events where $A > A_{max}$ with (e.g., *ID*1; **Supplementary Figure S2**) or without preceding contraction (e.g., *ID*2; **Supplementary Figure S2**). Expansions in the relative projected area A_r were significantly faster than contractions (GLMM, $t = -4.595$, $P = 4.3 \times 10^{-6}$), as expressed by mean (±$CI_{95\%}$) contraction v_C and expansion speeds v_E of -0.001 ± 0.001 ΔA_r min^{-1} and 0.004 ± 0.001 ΔA_r min^{-1}, corresponding to decreases of 7.0 ± 4.0% A_r h^{-1} and increases of 21.8 ± 6.5% A_r h^{-1}, respectively (**Table 1**).

DISCUSSION

Relationship Between Contractile Behavior and Respiration Rate

Our findings suggest that the respiration rate of single-osculum *H. panicea* explants is marginally affected by contractile behavior as respiration rates decreased by only ∼10% during non-pumping periods despite osculum closure for up to 131 min (cf. *ID*1, **Figure 2** and **Table 1**, contraction-expansion event #6 therein).

During periods of maximal water pumping activity, the advective flux through the water canal system of a sponge results in an internal oxygen concentration approaching that of the ambient seawater (**Figure 4A**; Hoffmann et al., 2005b, 2007; Schläppy et al., 2010b). In this case, fully oxygenated water (compared to what is in the environment) can saturate the water canal system providing maximum concentrations of oxygen to respiring cells (both sponge cells and prokaryotic cells of the microbiome), thus reducing the concentration gradient across the outer sponge tissues generating a small diffusive flux of oxygen across the external sponge surface (Hoffmann et al., 2008). In contrast, during pumping cessation, molecular diffusion across the outer-sponge body is the only mechanism for oxygen supply to the interior of the sponge (**Figure 4B**; Hoffmann et al., 2005a,b, 2008; Schläppy et al., 2007, 2010b). Osculum closure traps seawater in the water canal system, resulting in a loss of oxygen by respiration in the sponge interior (Hazelhoff, 1938). Reduced oxygen concentration in the sponge interior increases the oxygen gradient across the sponge surface and thus enhances the oxygen flux from the external environment into the sponge interior (**Figure 4B**; Hoffmann et al., 2005b; Schläppy et al., 2007, 2010b). This increase in oxygen flux across the sponge surface likely explains why the sponge only experiences a small decrease of ∼10% in the overall respiration rate in comparing when the osculum is open or closed. During osculum closure, the respiratory needs of the sponge, which have only slightly been changed, are met by diffusion through the outer sponge surface (**Figure 4B**).

For our hemispherical explants with a mean radius $r = 0.35$ cm, the (outer) respiratory surface area can be estimated as $A_{sp} = 2\pi r^2 = 0.77$ cm^2. The measured mean respiration rate hence corresponds to a diffusive flux J (= 0.046 μmol O_2 h^{-1}/0.77 cm^2 = 0.060 μmol O_2 $cm^{-2}h^{-1}$) = 1.44 μmol O_2 cm^{-2} d^{-1} across this surface area during periods of osculum closure. This value is in the range of previous measured oxygen fluxes in other sponge species, which exhibit internal anoxia during

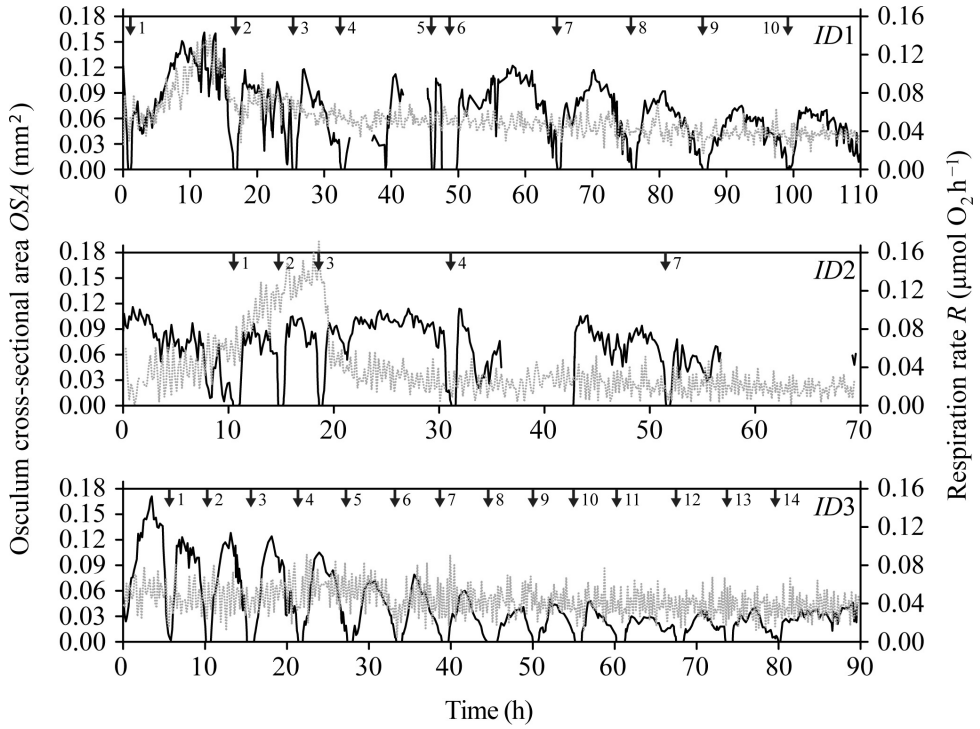

FIGURE 2 | *Halichondria panicea*. Simultaneous measurement of osculum cross-sectional osculum area (*OSA*, mm^2; dark line), and respiration rate (*R*, µmol O_2 h^{-1}; gray dashed line) of sponge explants (*ID*1 to *ID*3) as a function of time during respiration experiments with combined time-lapse observations of the explant osculum and body (**Figure 1**). Numbered arrows indicate contraction-expansion events (**Table 1**). Corresponding temporal changes in projected area (*A*) are given in **Supplementary Figure S2**.

pumping cessation (Hoffmann et al., 2005a, 2008). Assuming internal anoxia for our non-pumping *H. panicea* explants, a maximum oxygen gradient between ambient seawater and internal tissue $dC = 0.271\ \mu mol\ O_2\ cm^{-3}$ may be estimated from the mean initial oxygen concentration in our experiments. Fick's first law $J = -D \times dC/dx$ (Jørgensen and Revsbech, 1985; Hoffmann et al., 2008) applied with a diffusion coefficient $D = 1.52\ cm^2\ d^{-1}$ for oxygen in seawater at 15°C and 20 PSU (Ramsing and Gundersen, 2000, Table 1 therein) as an approximation for sponge tissue (cf. Hoffmann et al., 2008), a maximum penetration depth of oxygen into the sponge tissue can be calculated as $dx = [-(1.52\ cm^2\ d^{-1} \times 0.271\ \mu mol\ O_2\ cm^{-3})/1.44\ \mu mol\ O_2\ cm^2\ d^{-1}] = -0.29$ cm. Our single-osculum explants have a radius of 0.35 cm suggesting complete internal oxygen depletion under steady-state conditions. Oxygen depletion and the subsequent increase in the diffusive flux of oxygen across the sponge outer surface facilitates oxygenation of major parts of sponge tissue. Our findings emphasize that respiration rates during pumping cessation are controlled by the passive diffusive flux across the outer sponge surface (Hoffmann et al., 2008).

Considering the very small volume (V_{sp} = 0.09 cm^3) of our sponge explants as a lower size limit that allows for active filter-feeding, internal anoxia is likely to occur in larger demosponges showing pronounced non-pumping periods. The present single-osculum *H. panicea* explants revealed volume- and *DW*-specific respiration rates within the range of larger *H. panicea* specimens with multiple oscula and other sponge species (Thomassen and Riisgård, 1995; Osinga et al., 1999; Coma et al., 2002; Hadas et al., 2008; Hoffmann et al., 2008; Mills et al., 2014).

A comparable total oxygen consumption rate of 9.07 µmol O_2 d^{-1} $cm^{-3}{}_{sponge}$ was estimated for 10 day-old *Geodia baretti* explants without osculum (Hoffmann et al., 2005a) where oxygen must have been wholly supplied by diffusion across the outer sponge surface. However, unlike in the present experiments, a much higher reduction of ∼25% in respiration rates was observed for the coral reef sponge *Negombata magnifica* during reduced pumping activity (Hadas et al., 2008). Furthermore, in large (V_{sp} = 70 cm^3) *Aplysina aerophoba* sponges, respiration rate may decrease by up to 80% during pumping cessation (Hoffmann et al., 2008).

Such distinct differences in the respiration rate between pumping and non-pumping sponges for some species may reflect limitations of the diffusive oxygen flux across the sponge surface to sufficiently supply larger sponge volumes during periods of pumping cessation. Another explanation for the observed relatively small change in respiration of our explants could be the low metabolic cost for pumping in *H. panicea*, which has been estimated to ∼2% of the total oxygen consumption (Riisgård et al., 1993; but see also Riisgård and Larsen, 2016). In other demosponge species, such as *N. magnifica*, pumping costs can be considerably higher (e.g., 25 and 28% in *N. magnifica*

TABLE 1 | *Halichondria panicea*.

ID	C/E #	*t* (min)	Δt (min)	Δt_C (min)	Δt_P (min)	R_C (μmol $O_2 h^{-1}$)	R_P (μmol $O_2 h^{-1}$)	v_C (ΔOSA_r min^{-1})	v_E (ΔOSA_r min^{-1})	v_C (ΔA_r h^{-1})	v_E (ΔA_r h^{-1})
*ID*1	1	50	–	20	49	0.042	0.051	−0.022	0.010	−0.129	0.528
	2	991	941	30	920	0.068	0.087	−0.011	0.011	−0.128	0.351
	3	1516	525	33	494	0.060	0.069	−0.052	0.020	−0.042	0.238
	4	1952	436	30	402	0.054	0.058	−0.004	0.009	−0.120	0.233
	5	2763	811	21	780	0.044	0.052	−0.024	0.070	−0.002	0.181
	6	2853	90	131	68	0.053	0.053	−0.066	0.021	−0.028	0.018
	7	3891	1038	15	906	0.047	0.049	−0.003	0.012	−0.021	0.226
	8	4555	664	33	648	0.039	0.045	−0.004	0.010	−0.044	0.292
	9	5189	634	41	600	0.028	0.041	−0.004	0.008	−0.008	0.168
	10	5941	752	26	710	0.030	0.038	−0.003	0.014	−0.023	0.144
*ID*2	1	627	–	33	626	0.061	0.040	−0.041	0.136	−0.002	0.117
	2	884	257	26	223	0.111	0.095	−0.122	0.072	−0.011	0.133
	3	1116	232	19	205	0.132	0.133	−0.049	0.031	−0.005	0.153
	4	1870	754	24	734	0.023	0.036	−0.017	0.062	−0.010	0.162
	5	–	–	–	–	–	–	–	–	−0.004	0.345
	6	–	–	–	–	–	–	–	–	−0.006	0.426
	7	3093	1223	22	528	0.012	0.023	−0.011	0.025	−0.004	0.077
*ID*3	1	350	–	0	349	–	0.050	−0.015	0.015	−0.008	0.105
	2	607	257	35	256	0.043	0.046	−0.010	0.010	−0.073	0.386
	3	907	300	51	264	0.039	0.048	−0.007	0.008	−0.029	0.408
	4	1283	376	32	324	0.047	0.051	−0.005	0.008	−0.119	0.163
	5	1642	359	39	326	0.054	0.058	−0.005	0.006	−0.051	0.236
	6	2001	359	41	319	0.024	0.051	−0.006	0.013	−0.049	0.272
	7	2337	336	45	294	0.044	0.044	−0.006	0.007	−0.109	0.154
	8	2666	329	73	283	0.039	0.044	−0.006	0.003	−0.077	0.156
	9	3001	335	39	261	0.043	0.045	−0.013	0.010	−0.203	0.116
	10	3310	309	48	269	0.035	0.041	−0.006	0.020	−0.145	0.199
	11	3612	302	62	253	0.036	0.042	−0.004	0.011	−0.208	0.166
	12	4050	438	54	375	0.034	0.040	−0.004	0.008	−0.167	0.163
	13	4412	362	52	307	0.036	0.038	−0.004	0.011	−0.124	0.199
	14	4800	388	13	335	0.040	0.036	−0.005	0.004	−0.236	0.233
Mean			493	37.5	417.5	0.047	0.052	−0.018	0.022	−0.070	0.218
($\pm CI_{95\%}$)			($\pm$160)	($\pm$13.7)	($\pm$134)	($\pm$0.014)	($\pm$0.012)	($\pm$0.015)	($\pm$0.016)	($\pm$0.016)	($\pm$0.065)

*Contraction (C)-expansion (E) events (#1 to #14) during respiration experiments with combined time-lapse observations of the osculum cross-sectional area (OSA) and projected area (A) of sponge explants (ID1 to ID3) on glass slides in 0.2 μm filtered seawater (**Figure 2** and **Supplementary Figure S2**). t: time of osculum closure (OSA = 0 mm^2), Δt: time interval until subsequent osculum closure, Δt_C: duration of osculum closure, Δt_P: duration of active water pumping (OSA > 0 mm^2) until osculum closure, R_C and R_P: mean respiration rate during periods of osculum closure or active pumping, respectively, determined from the slope of linear regressions of the dissolved oxygen concentration over time (**Supplementary Figure S1**), v_C and v_E: contraction and expansion speed, respectively, estimated from the slope of linear regressions of the relative osculum cross-sectional area ($OSA_r = OSA/OSA_{max}$, **Figure 2**) or relative projected area over time ($A_r = A/A_{max}$, **Supplementary Figure S2**).*

and *Aphrocallistes vastus*, respectively; Hadas et al., 2008; Leys et al., 2011). While reduced pumping rates have previously been suggested as an energy-saving mechanism during periods of low food availability (Ludeman et al., 2017), the present findings indicate a minor role of contractile behavior for reducing the energetic demands of *H. panicea*.

Contraction-Expansion Behavior in Single-Osculum *Halichondria panicea* Explants

Osculum dynamics are characterized by cycles of contraction, closure and expansion of the oscular opening, with osculum contraction and expansion showing comparable speeds (**Table 1**). Assuming a circular osculum with a diameter of ($2 \times \sqrt{OSA_{max} \times \pi}$ =) 1.37 mm, and using a mean ($\pm CI_{95\%}$) relative contraction speed of -0.018 $\pm$ 0.015 ΔOSA_r min^{-1}, a mean osculum contraction speed of ($1.37 \times 0.018 \times 1000/60$ =) 0.41 $\mu m\ s^{-1}$ can be calculated. To our knowledge, this is the first estimate of the speed of natural (i.e., not stimulated) osculum contraction in a sponge. This value is much lower than typically observed in freshwater and other marine sponge species after electrical, chemical or mechanical stimulation of osculum contraction (McNair, 1923; Prosser et al., 1962; Emson, 1966). However, a contraction speed of 0.17 $\mu m\ s^{-1}$ has been observed after "very weak" electrical stimulation of the freshwater sponge *Ephydiatia fluviatilis* (cf. Figure 5 in McNair, 1923) which is comparable to our value for *H. panicea* explants.

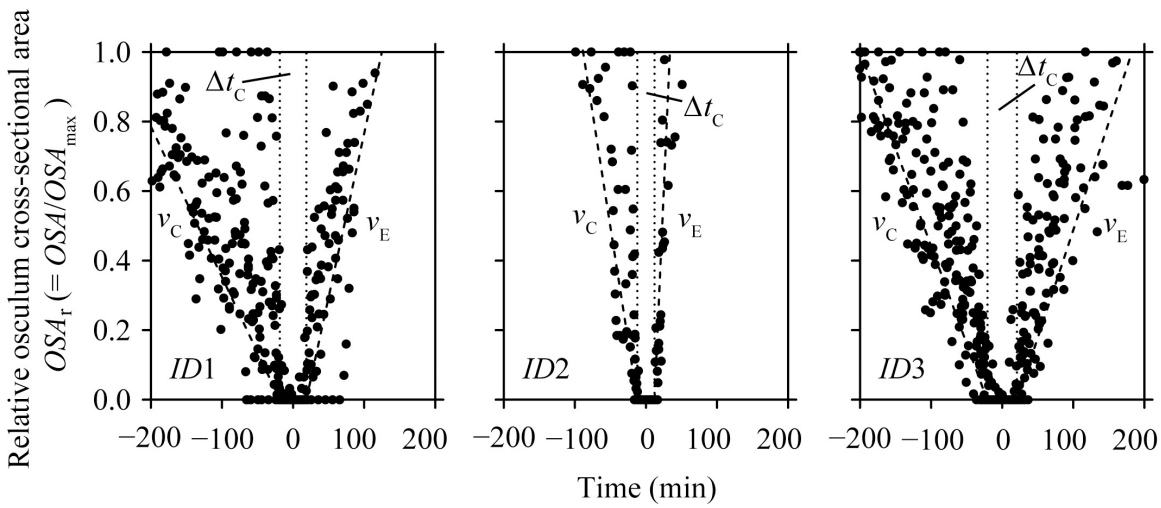

FIGURE 3 | *Halichondria panicea*. Relative osculum cross-sectional area (OSA_r, closed symbols) during contraction-expansion events of sponge explants (*ID*1 to *ID*3, **Table 1** and **Figure 2**) over time, where t_0 = 0 min is the mean time of osculum closure. Mean duration of osculum closure (Δt_C, dotted lines) and mean osculum contraction (v_C) and expansion (v_E) speeds (broken lines) are shown for each explant individual.

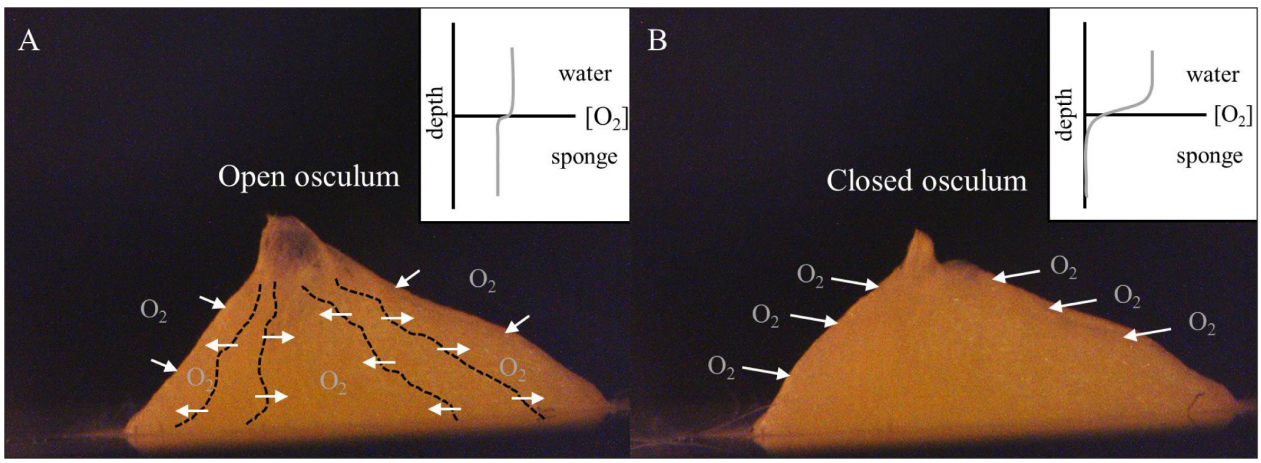

FIGURE 4 | *Halichondria panicea*. Schematic illustration of the oxygen regulation in single-osculum explants with **(A)** open and **(B)** closed osculum in continuously mixed filtered seawater (**Figure 1**). **(A)** Actively pumping sponges show a domination of advective oxygen transport via the water canal system (dashed lines), resulting in an internal oxygen concentration approaching that of the ambient seawater. **(B)** In contrast, non-pumping sponges typically show an enhanced diffusive boundary layer above their surface, and internal oxygen depletion (cf. Hoffmann et al., 2005b, 2008; Schläppy et al., 2007).

The sponge projected area, *A*, responds to changes in the *OSA*, including both small reductions and distinct expansions of *A* (**Figure 2** and **Supplementary Figure S2**). Changes in *A* during the contraction and expansion of our *H. panicea* explants were much less pronounced than have been observed in the demosponge *Tethya wilhelma* which demonstrates significant full body contractions, including constriction of the water canal system (Nickel, 2004; Ellwanger et al., 2007; Nickel et al., 2011). Further, *T. wilhelma* shows faster contraction than expansion of its projected area (Nickel, 2004) which is in contrast to our observations of significantly faster expansion than contraction in *H. panicea* explants. Generally, as previously suggested for sponges with rigid, spicule-rich skeletons (Nickel, 2010), contraction-expansion behavior in *H. panicea* is mainly expressed in contractions of the osculum as well as water canal system (cf. Kumala et al., 2017). The more pronounced body contractions (i.e., changes in *A*) in *T. wilhelma* probably reflect a larger collapse of the aquiferous system during contractions than for *H. panicea*.

We observed active pumping (i.e., $OSA > 0$ mm^2) of starved explants over extended periods Δt_P = 7.0 ± $CI_{95\%}$ 2.2 h and cyclic osculum closure for Δt_C = 37.5 ± $CI_{95\%}$ 13.7 min (**Table 1**). Similar contraction-expansion dynamics were observed for continuously fed *H. panicea* explants during laboratory experiments (Kumala et al., 2017) and other sponge species (e.g., *Verongia gigantea*) under natural conditions (Reiswig, 1971a). From a mean initial oxygen concentration of

271 μmol L^{-1} (i.e., 271 nmol cm^{-3}; **Supplementary Figure S1**) and a mean volume-specific respiration rate of 0.52 μmol O_2 h^{-1} cm^{-3}_{sponge} (i.e., 520 nmol O_2 $h^{-1}cm^{-3}_{sponge}$) as determined in the present study, an oxygen drawdown time, i.e., the time until complete reduction of oxygen within the sponge, of (271/520 =) 0.5 h can be estimated for the present *H. panicea* explants. This value is comparable to estimates for *A. aerophoba* which develops internal anoxic conditions within 15 min of pumping cessation (Hoffmann et al., 2008). In agreement with an oxygen penetration depth that is smaller than the dimensions of our sponge explants, a mean osculum closure time of 37.5 min as observed in the present study is likely to result in near of complete internal anoxia. In addition to osculum closure alone, associated sponge-body contractions can also expel water from the aquiferous system, as observed for the freshwater sponge *Ephydatia muelleri* (Elliott and Leys, 2007) and the marine sponge *T. wilhelma* (cf. Nickel, 2004). Thus, the oxygen drawdown time may become even shorter when seawater is expelled from the aquiferous system.

We observed individual differences in the contractile behavior of our explants, as expressed by irregular osculum contraction-expansion events in explants *ID*1 and *ID*2 as opposed to more frequent and regular events in explant *ID*3 (**Table 1** and **Figure 2**). Irregular events, which may indicate deviation from the regular contraction cycle (Reiswig, 1971a), were accompanied by an initial increase in the oxygen consumption (**Figure 2**; *ID*1 and *ID*2) but are most likely related to physiological disturbance/stress (e.g., due to transfer to respiration chamber; Peck and Conway, 2000), as emphasized by associated temporal increases in metabolic rates and nearly periodic contraction-expansion events in the second half of the experiments (**Figure 2**, *ID*1 and *ID*2). Temporal increases in oxygen uptake may also be related to digestion of symbiotic bacteria abundantly located in the sponge tissue, and to the oxidation of reduced compounds, such as ammonia which may internally accumulate as a waste product of the holobionts' metabolism (cf. Lavy et al., 2016).

Even though severe reductions in the ambient oxygen level may cause changes in the contraction rate of demosponges such as *T. wilhelma*, which changes its normal contraction behavior at oxygen concentrations below 4% air saturation (Mills et al., 2018), periodic osculum closure of our explants seems unlikely to be stress-related within the much higher investigated oxygen concentrations of 28–100% air saturation. Furthermore, there is evidence that environmental disturbances, such as resuspended sediment during storms or dredging, can also stimulate contractile behavior (Reiswig, 1971a; Pineda et al., 2017), which may include protection and cleaning of the filtration apparatus (Elliott and Leys, 2007; Tompkins-MacDonald and Leys, 2008). This was unlikely, however, in our experiments as the explants were maintained in (0.2 μm) filtered seawater throughout the experimental period.

Overall, we conclude that osculum contraction-expansion events and related pumping cessation follows a periodic pattern in *H. panicea* explants and may resemble an endogenously driven behavior.

The Nature of Pumping: Feeding or Ventilation?

The present study reveals that the sponge respiration is not appreciably affected by osculum dynamics and the pumping activity of *H. panicea* explants. Pumping dynamics do, however, influence filter-feeding (Kumala et al., 2017) and the internal redox state of the sponge body (Hoffmann et al., 2008). Both aerobic and anaerobic metabolic processes of associated microorganisms play an important role for several sponge species (Wilkinson and Fay, 1979; Weisz et al., 2007; Hoffmann et al., 2009; Maldonado et al., 2012; Lavy et al., 2016). Spatial and temporal oxygen depletion in the sponge body, as a consequence of changes in pumping activity (Schläppy et al., 2010b; Lavy et al., 2016), may maintain and regulate the activity of a highly diverse microbial consortia in sponges. This allows for efficient utilization and recycling of nutrients (Hoffmann et al., 2009) via alternating metabolic pathways. Nitrification and denitrification, for instance, have been observed in both high microbial abundance (HMA) and low microbial abundance (LMA) sponges (Schläppy et al., 2010a). The LMA sponge *H. panicea* may benefit from its associated microbes (Althoff et al., 1998; Wichels et al., 2006; Schneemann et al., 2010; Mills et al., 2014) by switching between oxic and anoxic internal oxygen conditions to maintain the activity of its microbiome utilizing waste products and recirculating nutrients within the sponge holobiont (Hoffmann et al., 2005b, 2009).

Recent studies showed a relationship between the filtration rate (F, mL min^{-1}) and the OSA (mm^2), which can be expressed as $F = 1.39 \times OSA$ (Kumala et al., 2017). Thus, for a mean maximum OSA_{max} = 0.149 mm^2 (n = 3 explants; **Figure 2**), a potential maximum filtration rate of F_{max} = (1.39 × 0.149 =) 0.21 mL min^{-1} can be estimated. Applying F_{max} to a mean explant DW of 6.4 × 10^{-3}g and a DW-specific respiration rate of 0.165 mL O_2 $h^{-1}g^{-1}$ DW_{sponge}, yields an F/R-ratio of [(0.21 × 60/1000)/(0.165 × 6.4 × 10^{-3}) =] 11.9 L H_2O (mL O_2)$^{-1}$ for the present single-osculum *H. panicea* explants. At air saturation (∼15°C and ∼20 PSU), the estimated F/R-ratio corresponds to a water volume of (11.9 × 6.6 =) 79 mL that must be passed through the explant for each mL oxygen consumed. Thus, during periods of maximal pumping activity, only (1/79 = 0.013 =) 1.3% of the oxygen is efficiently removed each time water is pumped through the sponge body. Sponges usually exhibit oxygen extraction efficiencies of a few percent (i.e., 1.1–5.6%; Yahel et al., 2003, Table 3 therein), which emphasizes that sponges respire only a small fraction of the oxygen supplied by water flow throughout the canal system (Hazelhoff, 1938; Reiswig, 1974).

Reducing the pumping rate to one-fifth of an undisturbed (=maximal) pumping *H. panicea* explant, for example, with constant respiratory demands, however, results in an increased extraction efficiency of still only 6.3%. This may explain why our explants (*ID*1 and *ID*3) were able to maintain constant respiration rates under reduced ambient oxygen levels despite the observed decrease in OSA_{max} in closed respiration chambers with decreasing oxygen concentrations over time (**Figure 2**

and **Supplementary Figure S1**). This emphasizes that sponges pump water at a high rate to satisfy their feeding requirements (Hazelhoff, 1938) and not to oxygenate their interiors, as this could be accomplished with considerably reduced pumping rates.

CONCLUSION

Osculum closure over extended time periods, as observed in the present study, can result in internal anoxia, hence resulting in enhanced diffusion of oxygen across the sponge surface which seems sufficient to cover the respiratory needs of our single-osculum *H. panicea* explants. We conclude that the degree of internal oxygen depletion is determined by the duration of osculum closure and depends on sponge size due to an oxygen consumption that is driven by physical characteristics rather than active processes. The present study indicates that contractile behavior is an intrinsically generated mechanism to control filter-feeding of sponges and to maintain the diverse microbial consortia inhabiting the sponge body. The present findings suggest that pumping water through the aquiferous system supplies sponges with food (Kumala et al., 2017) but may play a minor role for balancing respiratory demands.

ETHICS STATEMENT

The study was conducted on marine sponges (invertebrates) and therefore was exempted from this requirement.

AUTHOR CONTRIBUTIONS

LK and DEC conceived and designed the experiments and wrote the manuscript. LK performed the experiments and analyzed the data.

FUNDING

This work was supported by a scholarship (LK) from the Max-Planck Society (Max Planck Institute for Demographic Research, Germany), by a research grant (9278) from VILLUM FONDEN and by the Villum grant (Grant No. 16518; DEC).

ACKNOWLEDGMENTS

We thank Anni Glud and Morten Larsen for technical support, Lorenzo Rovelli and Josephine Goldstein for fruitful discussions, and Fernando Colchero for help with the statistical analyses. We also thank Hans Ulrik Riisgård, Gitai Yahel, and Brian Strehlow for constructive comments on an earlier version of the manuscript.

SUPPLEMENTARY MATERIAL

The Supplementary Material for this article can be found online at: https://www.frontiersin.org/articles/10.3389/fmars.2018.00410/full#supplementary-material

REFERENCES

Althoff, K., Schütt, C., Steffen, R., Batel, R., and Mueller, W. E. (1998). Evidence for a symbiosis between bacteria of the genus *Rhodobacter* and the marine sponge *Halichondria panicea*: harbor also for putatively toxic bacteria? *Mar. Biol.* 130, 529–536. doi: 10.1007/s002270050273

Bates, D., Maechler, M., Bolker, B., and Walker, S. (2015). Fitting linear mixed-effects models using lme4. *J. Stat. Softw.* 67, 1–48. doi: 10.18637/jss.v067.i01

Bergquist, P. R. (1978). *Sponges*. Berkeley: Press.

Brill, B. (1973). Untersuchungen zur ultrastruktur der choanocyte von *Ephydatia fluviatilis L. Z. Zellforsch. Mikrosk. Anat.* 144, 231–245. doi: 10.1007/BF00307304

Coma, R., Ribes, M., Gili, J. M., and Zabala, M. (2002). Seasonality of in situ respiration rate in three temperate benthic suspension feeders. *Limnol. Oceanogr.* 47, 324–331. doi: 10.4319/lo.2002.47.1.0324

Duckworth, A. R., and Pomponi, S. A. (2005). Relative importance of bacteria, microalgae and yeast for growth of the sponge *Halichondria melanadocia* (De Laubenfels, 1936): a laboratory study. *J. Exp. Mar. Biol. Ecol.* 323, 151–159. doi: 10.1016/j.jembe.2005.03.007

Elliott, G. R., and Leys, S. P. (2007). Coordinated contractions effectively expel water from the aquiferous system of a freshwater sponge. *J. Exp. Biol.* 210, 3736–3748. doi: 10.1242/jeb.003392

Ellwanger, K., Eich, A., and Nickel, M. (2007). GABA and glutamate specifically induce contractions in the sponge *Tethya wilhelma*. *J. Comp. Physiol A Neuroethol. Sens. Neural. Behav. Physiol.* 193, 1–11. doi: 10.1007/s00359-006-0165-y

Emson, R. H. (1966). The reactions of the sponge *Cliona celata* to applied stimuli. *Comp. Biochem. Physiol.* 18, 805–827. doi: 10.1016/0010-406X(66)90215-5

Fjerdingstad, E. J. (1961). The ultrastructure of choanocyte collars in *Spongilla lacustris* (L.). *Z. Zellforsch. Mikrosk. Anat.* 53, 645–657. doi: 10.1007/BF00339512

Gaino, E., Pansini, M., Pronzato, R., and Cicogna, F. (1991). "Morphological and structural variations in *Clathrina clathrus* (Porifera, Calcispongiae)," in *Fossil and Recent Sponges*, eds J. Reitner and H. Keupp (Berlin: Springer-Verlag), 360–371. doi: 10.1007/978-3-642-75656-6_28

Hadas, E., Ilan, M., and Shpigel, M. (2008). Oxygen consumption by a coral reef sponge. *J. Exp. Biol.* 211, 2185–2190. doi: 10.1242/jeb.015420

Hazelhoff, E. H. (1938). Über die ausnutzung des sauerstoffs bei verschiedenen wassertieren. *J. Comp. Physiol. A Neuroethol. Sens. Neural. Behav. Physiol.* 26, 306–327.

Hoffmann, F., Larsen, O., Rapp, H. T., and Osinga, R. (2005a). Oxygen dynamics in choanosomal sponge explants. *Mar. Biol. Res.* 1, 160–163. doi: 10.1080/17451000510019006

Hoffmann, F., Larsen, O., Thiel, V., Rapp, H. T., Pape, T., Michaelis, W., et al. (2005b). An anaerobic world in sponges. *Geomicrobiol. J.* 22, 1–10. doi: 10.1080/01490450590922505

Hoffmann, F., Radax, R., Woebken, D., Holtappels, M., Lavik, G., Rapp, H. T., et al. (2009). Complex nitrogen cycling in the sponge *Geodia barretti*. *Environ. Microbiol.* 11, 2228–2243. doi: 10.1111/j.1462-2920.2009.01944.x

Hoffmann, F., Røy, H., Bayer, K., Hentschel, U., Pfannkuchen, M., Brümmer, F., et al. (2008). Oxygen dynamics and transport in the mediterranean sponge *Aplysina aerophoba*. *Mar. Biol.* 153, 1257–1264. doi: 10.1007/s00227-008-0905-3

Hoffmann, F., Sauter, E., Sachs, O., Røy, H., and Klages, M. (2007). "Oxygen distribution in tentorium semisuberites and in its habitat in the arctic deep sea," in *Porifera Research: Biodiversity, Innovation, Sustainability*, eds M. Custódio,

G. Lôbo-Hajdu, E. Hajdu, and G. Muricy (Rio de Janeiro: Série Livros. Museu Nacional), 379–382.

Jones, W. C. (1962). Is there a nervous system in sponges? *Biol. Rev. Camb. Philos. Soc.* 37, 1–50. doi: 10.1111/j.1469-185X.1962.tb01602.x

Jørgensen, B. B., and Revsbech, N. P. (1985). Diffusive boundary layers and the oxygen uptake of sediments and detritus. *Limnol. Oceanogr.* 30, 111–122. doi: 10.4319/lo.1985.30.1.0111

Kilian, E. F. (1952). Wasserströmung und nahrungsaufnahme beim süsswasserschwamm ephydatia fluviatilis. *Z. Vgl. Physiol.* 34, 407–447. doi: 10.1007/BF00297877

Kumala, L., Riisgård, H. U., and Canfield, D. E. (2017). Osculum dynamics and filtration activity in small single-osculum explants of the demosponge *Halichondria panicea*. *Mar. Ecol. Prog. Ser.* 572, 117–128. doi: 10.3354/meps12155

Larsen, P. S., and Riisgård, H. U. (1994). The sponge pump. *J. Theor. Biol.* 168, 53–63. doi: 10.1006/jtbi.1994.1087

Lavy, A., Keren, R., Yahel, G., and Ilan, M. (2016). Intermittent hypoxia and prolonged suboxia measured in situ in a marine sponge. *Front. Mar. Sci.* 3:263. doi: 10.3389/fmars.2016.00263

Leys, S. P., Yahel, G., Reidenbach, M. A., Tunnicliffe, V., Shavit, U., and Reiswig, H. M. (2011). The sponge pump: the role of current induced flow in the design of the sponge body plan. *PLoS One* 6:e27787. doi: 10.1371/journal.pone.0027787

Ludeman, D. A., Reidenbach, M. A., and Leys, S. P. (2017). The energetic cost of filtration by demosponges and their behavioural response to ambient currents. *J. Exp. Biol.* 220, 995–1007. doi: 10.1242/jeb.146076

Maldonado, M., Ribes, M., and Van Duyl, F. C. (2012). "Nutrient fluxes through sponges: biology, budgets, and ecological implications," in *Advances in Sponge Science: Physiology, Chemical and Microbial Diversity, Biotechnology*, Vol. 62, eds M. A. Becerro, M. J. Uriz, M. Maldonado, and X. Turon (San Diego, CA: Elsevier Academic Press Inc), 113–182.

McMurray, S. E., Pawlik, J. R., and Finelli, C. M. (2014). Trait-mediated ecosystem impacts: how morphology and size affect pumping rates of the Caribbean giant barrel sponge. *Aquat. Biol.* 23, 1–13. doi: 10.3354/ab00612

McNair, G. T. (1923). Motor reactions of the fresh-water sponge *Ephydatia fluviatilis*. *Biol. Bull.* 44, 153–166. doi: 10.2307/1536773

Mills, D. B., Francis, W. R., Vargas, S., Larsen, M., Elemans, C. P., Canfield, D. E., et al. (2018). The last common ancestor of animals lacked the HIF pathway and respired in low-oxygen environments. *Elife* 7:e31176. doi: 10.7554/eLife.31176.00

Mills, D. B., Ward, L. M., Jones, C., Sweeten, B., Forth, M., Treusch, A. H., et al. (2014). Oxygen requirements of the earliest animals. *Proc. Natl. Acad. Sci. U.S.A.* 111, 4168–4172. doi: 10.1073/pnas.1400547111

Nickel, M. (2004). Kinetics and rhythm of body contractions in the sponge *Tethya wilhelma* (Porifera: Demospongiae). *J. Exp. Biol.* 207, 4515–4524. doi: 10.1242/jeb.01289

Nickel, M. (2010). Evolutionary emergence of synaptic nervous systems: what can we learn from the non-synaptic, nerveless Porifera? *Invertebr. Biol.* 129, 1–16. doi: 10.1111/j.1744-7410.2010.00193.x

Nickel, M., Donath, T., Schweikert, M., and Beckmann, F. (2006). Functional morphology of *Tethya* species (Porifera): 1. *Quantitative* 3D-analysis of *Tethya wilhelma* by synchrotron radiation based X-ray microtomography. *Zoomorphology* 125, 209–223. doi: 10.1007/s00435-006-0021-1

Nickel, M., Scheer, C., Hammel, J. U., Herzen, J., and Beckmann, F. (2011). The contractile sponge epithelium sensu lato–body contraction of the demosponge *Tethya wilhelma* is mediated by the pinacoderm. *J. Exp. Biol.* 214, 1692–1698. doi: 10.1242/jeb.049148

Osinga, R., Tramper, J., and Wijffels, R. H. (1999). Cultivation of marine sponges. *Mar. Biotechnol.* 1, 509–532. doi: 10.1007/PL00011807

Patterson, M. R., Chernykh, V. I., Fialkov, V. A., and Savarese, M. (1997). Trophic effects of sponge feeding within Lake Baikal's littoral zone. 1. In situ pumping rates. *Limnol. Oceanogr.* 42, 171–178. doi: 10.4319/lo.1997.42.1.0171

Pavans de Ceccatty, M. (1974). Coordination in sponges. The foundations of integration. *Am. Zool.* 14, 895–903. doi: 10.1093/icb/14.3.895

Pavans de Ceccatty, M. (1986). Cytoskeletal organization and tissue patterns of epithelia in the sponge *Ephydatia mülleri*. *J. Morphol.* 189, 45–65. doi: 10.1002/jmor.1051890105

Pavans de Ceccatty, M. (1989). Les éponges, à l'aube des communications cellulaires. *Pour. Sci.* 142, 64–72.

Peck, L. S., and Conway, L. Z. (2000). "The myth of metabolic cold adaptation: oxygen consumption in stenothermal antarctic bivalves," in *The Evolutionary Biology of the Bivalvia*, Vol. 177, eds E. Harper, J. D. Taylor, and J. A. Crame (London: Geological Society, Special Publications), 441–450.

Pile, A. J., Patterson, M. R., Savarese, M., Chernykh, V. I., and Fialkov, V. A. (1997). Trophic effects of sponge feeding within Lake Baikal's littoral zone. 2. sponge abundance, diet, feeding efficiency, and carbon flux. *Limnol. Oceanogr.* 42, 178–184. doi: 10.4319/lo.1997.42.1.0178

Pineda, M. C., Strehlow, B., Kamp, J., Duckworth, A., Jones, R., and Webster, N. S. (2017). Effects of combined dredging-related stressors on sponges: a laboratory approach using realistic scenarios. *Sci. Rep.* 7:5155. doi: 10.1038/s41598-017-05251-x

Prosser, C. L., Nagai, T., and Nystrom, R. A. (1962). Oscular contractions in sponges. *Comp. Biochem. Physiol.* 6, 69–74. doi: 10.1016/0010-406X(62)90044-0

R Core Team (2015). *R: A Language and Environment for Statistical Computing*. Vienna: R Foundation for Statistical Computing.

Ramsing, N., and Gundersen, J. (2000). *Seawater and Gases: Tabulated Physical Parameters of Interest to People Working with Microsensors in Marine Systems. Unisense*. Available at: http://www.unisense.com/files/PDF/Diverse/Seawater%20&%20Gases%20table.pdf

Reiswig, H. M. (1971a). In situ pumping activities of tropical Demospongiae. *Mar. Biol.* 9, 38–50. doi: 10.1007/BF00348816

Reiswig, H. M. (1971b). Particle feeding in natural populations of three marine demosponges. *Biol. Bull.* 141, 568–591. doi: 10.2307/1540270

Reiswig, H. M. (1974). Water transport, respiration and energetics of three tropical marine sponges. *J. Exp. Mar. Biol. Ecol.* 14, 231–249. doi: 10.1016/0022-0981(74)90005-7

Riisgård, H. U., Kumala, L., and Charitonidou, K. (2016). Using the F/R-ratio for an evaluation of the ability of the demosponge *Halichondria panicea* to nourish solely on phytoplankton versus free-living bacteria in the sea. *Mar. Biol. Res.* 12, 907–916. doi: 10.1080/17451000.2016.1206941

Riisgård, H. U., and Larsen, P. S. (2000). Comparative ecophysiology of active zoobenthic filter-feeding, essence of current knowledge. *J. Sea Res.* 44, 169–193. doi: 10.1016/S1385-1101(00)00054-X

Riisgård, H. U., and Larsen, P. S. (2016). Comments on Leys et al. (2011) "The sponge pump: the role of current induced flow in the design of the sponge body plan". *PLoS One* 6:1–17. doi: 10.13140/RG.2.1.3673.7687

Riisgård, H. U., Thomassen, S., Jakobsen, H., Weeks, J., and Larsen, P. S. (1993). Suspension feeding in marine sponges *Halichondria panicea* and *Haliclona urceolus*: effects of temperature on filtration rate and energy cost of pumping. *Mar. Ecol. Prog. Ser.* 96, 177–188. doi: 10.3354/meps096177

Schläppy, M. L., Hoffmann, F., Røy, H., Wijffels, R. H., Mendola, D., Sidri, M., et al. (2007). Oxygen dynamics and flow patterns of *Dysidea avara* (Porifera: Demospongiae). *J. Mar. Biol. Assoc. U.K.* 86, 1677–1682. doi: 10.1017/S0025315407058146

Schläppy, M. L., Schöttner, S. I., Lavik, G., Kuypers, M. M., de Beer, D., and Hoffmann, F. (2010a). Evidence of nitrification and denitrification in high and low microbial abundance sponges. *Mar. Biol.* 157, 593–602. doi: 10.1007/s00227-009-1344-5

Schläppy, M. L., Weber, M., Mendola, D., Hoffmann, F., and de Beer, D. (2010b). Heterogeneous oxygenation resulting from active and passive flow in two Mediterranean sponges, Dysidea avara and Chondrosia reniformis. *Limnol. Oceanogr.* 55, 1289–1300. doi: 10.4319/lo.2010.55.3.1289

Schneemann, I., Nagel, K., Kajahn, I., Labes, A., Wiese, J., and Imhoff, J. F. (2010). Comprehensive investigation of marine Actinobacteria associated with the sponge *Halichondria panicea*. *Appl. Environ. Microbiol.* 76, 3702–3714. doi: 10.1128/AEM.00780-10

Strehlow, B. W., Jorgensen, D., Webster, N. S., Pineda, M. C., and Duckworth, A. (2016). Using a thermistor flowmeter with attached video camera for monitoring sponge excurrent speed and oscular behaviour. *PeerJ* 4:e2761. doi: 10.7717/peerj.2761

Taylor, M. W., Radax, R., Steger, D., and Wagner, M. (2007). Sponge-associated microorganisms: evolution, ecology, and biotechnological potential. *Microbiol. Mol. Biol. Rev.* 71, 295–347. doi: 10.1128/MMBR.00040-06

Thomas, T., Moitinho-Silva, L., Lurgi, M., Björk, J. R., Easson, C., Astudillo-García, C., et al. (2016). Diversity, structure and convergent evolution of the global sponge microbiome. *Nat. Commun.* 7:11870. doi: 10.1038/ncomms11870

Thomassen, S., and Riisgård, H. U. (1995). Growth and energetics of the sponge *Halichondria panicea*. *Mar. Ecol. Prog. Ser.* 128, 239–246. doi: 10.3354/meps128239

Tompkins-MacDonald, G. J., and Leys, S. P. (2008). Glass sponges arrest pumping in response to sediment: implications for the physiology of the hexactinellid conduction system. *Mar. Biol.* 154, 973–984. doi: 10.1007/s00227-008-0987-y

Weisz, J. B., Hentschel, U., Lindquist, N., and Martens, C. S. (2007). Linking abundance and diversity of sponge-associated microbial communities to metabolic differences in host sponges. *Mar. Biol.* 152, 475–483. doi: 10.1007/s00227-007-0708-y

Wichels, A., Würtz, S., Döpke, H., Schütt, C., and Gerdts, G. (2006). Bacterial diversity in the breadcrumb sponge *Halichondria panicea* (Pallas). *FEMS Microbiol. Ecol.* 56, 102–118. doi: 10.1111/j.1574-6941.2006.00067.x

Wilkinson, C. R., and Fay, P. (1979). Nitrogen fixation in coral reef sponges with symbiotic cyanobacteria. *Nature* 279, 527–529. doi: 10.1038/279527a0

Yahel, G., Sharp, J. H., Marie, D., Häse, C., and Genin, A. (2003). In situ feeding and element removal in the symbiont-bearing sponge *Theonella swinhoei*: bulk DOC is the major source for carbon. *Limnol. Oceanogr.* 48, 141–149. doi: 10.4319/lo.2003.48.1.0141

Conflict of Interest Statement: The authors declare that the research was conducted in the absence of any commercial or financial relationships that could be construed as a potential conflict of interest.